

Journal of Materials Chemistry A

Accepted Manuscript



This is an *Accepted Manuscript*, which has been through the Royal Society of Chemistry peer review process and has been accepted for publication.

Accepted Manuscripts are published online shortly after acceptance, before technical editing, formatting and proof reading. Using this free service, authors can make their results available to the community, in citable form, before we publish the edited article. We will replace this *Accepted Manuscript* with the edited and formatted *Advance Article* as soon as it is available.

You can find more information about *Accepted Manuscripts* in the [Information for Authors](#).

Please note that technical editing may introduce minor changes to the text and/or graphics, which may alter content. The journal's standard [Terms & Conditions](#) and the [Ethical guidelines](#) still apply. In no event shall the Royal Society of Chemistry be held responsible for any errors or omissions in this *Accepted Manuscript* or any consequences arising from the use of any information it contains.

Development of Zwitterionic Polyurethanes with Multi-Shape Memory Effects and Self-healing Properties

*Shaojun Chen**, *Funian Mo*, *Yan Yang*, *Florian-Johannes Stadler*, *Shiguo Chen*, *Haipeng Yang*, *Zaochuan Ge**,

Shenzhen Key Laboratory of Special Functional Materials, Nanshan District Key Lab for Biopolymers and Safety Evaluation, College of Materials Science and Engineering, Shenzhen University, Shenzhen, 518060, China.

E-mail: S.J.Chen, chensj@szu.edu.cn; Z.C.Ge gezgc@szu.edu.cn;

Abstract

Recently, multi-shape-memory polymers have attracted significant attention due to their technological impact. This paper reports novel zwitterionic multi-shape-memory polyurethanes (ZSMPUs) from N-methyldiethanolamine (MDEA), hexamethylene diisocyanate (HDI) and 1,3-propanesultone (PS). ZSMPUs feature excellent multi-shape-memory properties that are capable of remembering four different shapes, while shape recovery decreases with increasing sulfobetaine content. Ionic interactions greatly influence the structure, morphology and properties. Increasing sulfobetaine content promotes the phase mixing and zwitterions serve as organic fillers in the zwitterionic polyurethane. Immersing the zwitterionic polyurethane in moisture conditions and drying at low temperature preserves shape-memory capabilities and demonstrates good self-healing properties. Furthermore, both shape memory effect and self-healing effects are repeatable. The self-healing mechanism is ascribed to the spontaneous attraction of zwitterions, followed by slower re-entanglement.

Keywords: zwitterionic polymer; shape memory; self-healing; polyurethane; ionic interaction;

1. Introduction

Shape-memory polymers (SMPs) are gaining importance as smart biomaterials due to their capability to change shape in response to a desired stimulus.^{1,2} Recently developed multi-shape-memory polymers with the ability to sequentially recover their original shape *via* several previously programmed temporary shapes have significant technological impact.^{3,4} For biomedical applications, SMPs should also be biocompatible and have tunable actuation temperatures and glassy elastic moduli.^{5,6} Shape memory polyurethanes (SMPUs) have gained increasing attention recently, owing to their adjustable transition temperature and good biocompatibility.^{7,8} To date, many types of glycols including polycaprolactone diols (PCL), polylactic acid (PLA) and polyethylene glycol (PEG) have been used to synthesize SMPUs.⁹⁻¹¹ Potential biomedical applications of SMPs include endovascular stroke treatments, cardiac valve repair, and tissue engineering.¹²⁻¹⁵ The biocompatibility demonstrated by low cytotoxicity, low thrombogenicity, low platelet activation, low cytokine activation and low *in vivo* inflammatory response, are also reported for Diapplex SMPUs, PLA-SMPUs, and PCL-diacrylate SMPs.^{5,6} However, to date, only a few SMP-based biomedical devices have been commercialised. Even SMPUs based on the biocompatible PEG soft segments show low cell viability when containing above 40 wt.% hard segments.¹⁶ Thus, adding biocompatibility in addition to shape-memory functionality is quite necessary before using SMPs as medical implants or scaffolds in tissue engineering.⁵

As the introduction of zwitterionic groups or phosphorylcholine structures into polymers can enhance their biocompatibility,¹⁷ much attention has been focused on surface grafting zwitterionic groups.^{18, 19} Recently, polyurethanes containing zwitterionic groups were synthesized from the zwitterionically functionalised diols.²⁰⁻²² The introduction of zwitterionic sulfobetaine units into polyurethanes significantly improved hydrophilicity and reduced protein adsorption. Good blood compatibility, characterised by low hemolysis and delayed blood clotting, is achieved by such zwitterionic polyurethanes.²² Polyurethane based SMPs are usually block copolymers with soft and hard segments, with the latter acting as physical crosslinks, while the former yields a soft phase with a transition temperature above room temperature, serving as the reversible phase. Thus, designing and synthesizing novel zwitterionic polyurethanes with sulfobetaine groups is desirable for obtaining biocompatible SMPUs. Moreover, the zwitterionic polyurethanes are also expected to have tunable multi-shape memory effects^{23, 24}. Similar to the perfluorosulfonate ionomer and polyethylene-based carboxylated ionomer,^{4, 25} the ionic clusters may provide multifunctional physical crosslinks within amorphous phase and the sulfobetaine long side chains endow the polymer with broad transition.

In this paper, we propose a novel strategy to prepare zwitterionic shape memory polyurethanes (ZSMPUs), using zwitterionic polyurethanes with suitable transition temperatures, prepared by two-step reactions. Unlike previous SMPU and common zwitterionic polyurethane systems,²⁰⁻²² ZSMPUs are synthesized with N-methyldiethanolamine (MDEA) and hexamethylene diisocyanate (HDI), followed by grafting of zwitterionic side-chains onto the backbone by ring-opening reaction of 1,3-propanesultone (PS), thus forming zwitterionic units (MDEAPS). The transition temperature is altered by the sulfobetaine content, which also affects the biocompatibility needed in biomedical applications. The synthesized ZSMPUs are able to remember two to four shapes. Additionally, ZSMPUs are also self-healing.

2. Experimental

2.1 Materials

Raw materials including N-methyldiethanolamine (MDEA, analytic grade), hexamethylene diisocyanate (HDI, analytic grade), 1,3-propanesultone (PS, analytic grade), Dibutyltin dilaurate (DBTD, analytic grade, catalyst for polyurethane polymerisation), and Dimethylformamide (DMF, High Performance Liquid Chromatography grade, solvent) were purchased from Aladdin (Shanghai, China).

2.2 Preparation

Table 1

Scheme 1

A series of ZSMPU samples with different MDEAPS-content were synthesized by adjusting the PS/MDEA molar ratios varied from 0.2–0.8 (**Table 1**) and using polyurethane polymerization followed by the ring-opening reaction method. The synthetic route of ZSMPU is presented in **Scheme 1**. The preparation of the polyurethane pre-polymer was performed in a nitrogen filled and mechanically stirred 500 ml three-neck flask. For the first polyurethane polymerisation step, 34.5 g HDI, 20.0 g MDEA, 100 ml DMF, and 0.02 wt.% catalyst (DBTD) were added sequentially under vigorous stirring. The reaction started immediately when the temperature was increased to ca. 80°C. The reaction progress was obvious due to a significant increase in viscosity. Occasionally during the reaction, 10 ml DMF was added into the reaction to control the solution viscosity. For the second step, the ring-opening reaction, 30 g of the synthesized polyurethane prepolymer in DMF (e.g., 10wt.%) was reacted with PS (e.g., 0.294 g) in an Erlenmeyer flask according to the molar ratio of PS/MDEA (**Table 1**). The reaction was performed hermetically at 50°C for 12 hours. Finally, DMF was evaporated from the resulting 10 wt.% ZSMPU/DMF solution in a Teflon pan at 80°C for 24 hours in continuous air flow and then *in vacuum* for another 24 hours. In this study, the sample names of ZSMPUs were coded as ZSMPU#, in which “#” refers to the PS/MDEA molar ratio divided by 10, e.g. ZSMU4.

2.3 Characterization

ATR-FTIR spectra were recorded with a Nicolet 760 FT-IR spectrometer equipped with an ATR accessory MUP with GeS crystal. 24 scans at 4 cm⁻¹ resolution were signal averaged and stored as data files for further analysis.

The ¹H-NMR spectrum was recorded with Avance-400Hz (Bruker) with D₇-DMF as the solvent and tetramethylsilane (TMS) as internal standard.

The weight percentages of C, H, N and S of the ZSMPU were determined using a Vario EL III elemental analyzer (EA, Germany Elementar).

The XPS analysis was made on a VG multilab2000 with Al Ka source. The anode voltage was 15KV and the anode current was 10mA. The core-level signals were obtained at a photoelectron take-off angle of 90°. The elemental compositions were determined on the basis of peak areas and sensitivity factor from the C_{1s}, N_{1s}, O_{1s} and S_{2p} peaks by advantage software. All binding energy values were determined with reference to carbon, C_{1s}=284.6eV.

DSC testing was carried out by using a TA Q200 instrument having nitrogen as the purged gas. Indium and zinc standards were used for calibration. Samples were firstly heated up from -60 °C to 150°C at a heating rate of 10°C/min and kept at 150 °C for 1 min, subsequently, cooled to -60°C at a cooling rate of 10°C/min, and

finally the second heating scan from -60°C to 150°C was performed again.

TGA curves were recorded after drying at 100°C on a computer-controlled TA Instrument TG Q50 system, under the following operational conditions: heating rate $10^{\circ}\text{C}/\text{min}$, temperature range $100\text{--}600^{\circ}\text{C}$, sample weight about 5.0mg , using the film sample in platinum crucibles, $60\text{ ml}/\text{min}$ N_2 flow. Three or four repeated readings (temperature and weight loss) were performed on the same TG curve, each of them having at least 15 points.

Modulus testing was carried out by a computer-controlled TA Instrument DMA800 system. Specimens were cut from sample film with thickness of 0.5 mm , and the distance between two clamps is 10 mm in the initial testing status. Specimens were determined under 1.0 Hz and a heating rate of $2.0\text{ K}/\text{min}$.

Nanonavi E-Sweep (SII Nanotechnology Inc.) atomic force microscopy (AFM) was used in tapping mode for morphological characterization of the dried sample. The samples were dissolved in DMF at a concentration of $5\text{ mg}/\text{ml}$ and spin-coated firstly at 400 rpm for 10 s and then 4000 rpm for 60 s on oxidized silicon substrates. Spin-coated films were kept in a 50°C oven for 48 h to evaporate the solvent.

Static contact angle measurements were performed on a JC2000Y stable contact angle analyzer (China) at room temperature with distilled water as test liquid. With each specimen, the measurements were repeated at three different locations.

The moisture absorption was determined by weighing the specimens on a balance, referring the literature²⁶. Before testing, the specimens with a thickness of 1.0 mm were dried completely. The specimen was then put on the moisture condition with a certain RH and a certain temperature. The moisture absorption in percentage at any time (M_t) is calculated with the increased weight by comparing with the weight of dry sample.

The tensile mechanical-properties were investigated with an Instron 4465 testing machine. Elongation rate was set to $10\text{ mm}/\text{min}$. The specimens were rectangle ($20\text{ mm} \times 4\text{ mm} \times 0.5\text{ mm}$). Strain-stress curves are recorded for analysis.

The thermal-induced shape-memory behaviours were determined with thermo-mechanical analysis using a DMA800 instrument (tension clamp, controlled force mode) according the procedure described in literatures^{3, 4, 27}. The detail test setup for dual-shape-memory cycles, triple-shape-memory cycles and quadruple-shape-memory cycles are provided in supporting information (**Test S1**). Shape fixity and shape recovery was used to characterize the effectiveness at fixing temporary shape and the effectiveness of the shape recovery in each step^{4, 28, 29}, the detail calculations are provided in supporting information²⁵ (**Test S1**).

Specimens for self-healing and repeated healing were treated as below (**Scheme 2**), a typical sample, e.g.

ZSMPU8, was cut into three rectangle film. One film was treated directly by immersing at 80%RH and drying at 50°C. The resulted specimen is coded as ZSMPU8-0 for the original sample. The second film was first cut into two parts on the middle. The two parts were treated by firstly immersing at 80%RH for 30mins; and the two parts was then recombined into a rectangle film. After drying at 50°C, the second specimen was coded as ZSMPU8-1 for the first healed sample. Similarly, the third film was also first cut into two parts on the middle. The two parts were treated by firstly immersing at 80%RH for 30mins; and the two parts was then recombined into a rectangle film. After drying at 50°C, the recombine film was exactly cut into two parts again on the recombine-position (on the middle); and the two parts was treated again by secondly immersing 80%RH for another 30mins. The two parts was then recombined into a rectangle film. After the secondly drying at 50°C, the resulted specimen was coded as ZSMPU8-2 for the second healed sample.

3. Results and Discussion

3.1 Structure analysis

Figure 1.

The bulk elemental compositions of samples were determined, and the real content of sulfobetaine was calculated based on sulfur content (Table 1), which is lower than the theoretical content, possibly due to incomplete ring-opening reactions or decomposition of MDEAPS during storing or drying. Table 1 clearly demonstrates that the incorporated sulfobetaine increases as the theoretical ratio of PS/MDEA increases, confirming the success of zwitterions grafting on the polyurethanes scaling in a meaningful fashion with the theoretical composition. The molecular structure of the polyurethane prepolymer (ZSMPU0) and zwitterionic polyurethanes was systematically investigated with ATR-FTIR, ¹H-NMR and XPS (Figure 1). The broad shoulder at 3318 cm⁻¹, corresponding to N-H stretching vibration and the characteristic carbonyl peaks at 1688 cm⁻¹, indicates the formation of urethane linkages in ZSMPU0 (Figure 1A). The peak appearing at 1038 cm⁻¹ suggests the presence of SO₃⁻ groups and the weak vibration, corresponding to the quaternary N-group, is also detected at 960 cm⁻¹ in ZSMPU4. This finding confirms the grafting of sulfobetaine onto the backbone of polyurethane in the second reaction step. ¹H-NMR spectra further show additional chemical shifts at 3.10 ppm in ZSMPU4, assigned to the methyl proton signal of >N⁺-CH₃. There are also some new chemical shift bands at 1.70 ppm, 2.77 ppm, and 3.67 ppm, ascribed to the proton signals from the -CH₂ of the sulfobetaine groups. Moreover, when compared to ZSMPU0 and after grafting the sulfobetaine groups, the -CH₂ of the MDEA groups (at 3.98 ppm) in ZSMPU4 shift to higher chemical shifts, e.g., 4.16 ppm and 4.36 ppm. The chemical shifts of N-H at approximately 8.0 ppm in the ZSMPU0 also shift to another chemical shift at approximately 7.2

~7.4 ppm due to the influence of sulfobetaine groups (**Figure 1B**). Additionally, the XPS survey scan spectra proves the existence of S_{2s} (binding energy, 230eV) and S_{2p} (binding energy, 166eV) orbitals in ZSMPU4 but not in ZSMPU0, which is indicative atoms of sulfobetaine (**Figure 1C**). Furthermore, the N_{1s} spectrum of the ZSMPU4 consists of two peaks, 402 eV from sulfobetaine's ternary ammonium ($>N^+-CH_3$) and 400 eV for the urethane nitrogen ($-N-COO$)¹⁸ or unmodified $>N-CH_3$ groups, which are also found for the ZSMPU0 (**Figure 1D**). The C_{1s} fine scan spectrum also shows three main peaks with 284.8, 285.9, and 288.8 eV of binding energy, corresponding to alkylic carbons ($-C-C-$), carbons singly bonded to oxygen ($-C-O-$) or carbons bonded to nitrogen ($-C-N-$), or carbons bonded to-sulfur ($-C-S-$), or carbonyl carbon atoms ($-C=O-$)³⁰ (**Figure S1**), respectively. This finding also confirms that sulfobetaine was successfully grafted onto polyurethane. Additionally, FT-IR spectra demonstrate that the N-H stretching vibration frequency (at 3318 cm^{-1}) shifts to a lower frequency due to moisture absorption in ZSMPU4 in comparison to ZSMPU0 (**Figure 1A**). As the MDEAPS-content increases, the frequency of the $-C=O$ stretching vibration in the zwitterionic polyurethanes increases linearly from ZSMPU0 (at 1689 cm^{-1}) to ZSMPU8 (at 1702 cm^{-1}) (**Figure S2**), implying that the hydrogen bonding of urethane groups becomes weaker as MDEAPS-content increases. The formation of sulfobetaine groups may destroy the intermolecular action of urethane groups, which can serve as physical cross-linkers for the shape-memory effects in the zwitterionic polyurethane.

3.2 Thermal-properties

Figure 2.

Thermal-properties including thermal phase transition and thermal-stability are investigated systematically with DSC and TG. **Figure 2A** demonstrates that all polyurethanes including the polyurethane prepolymer and zwitterionic polyurethanes form an amorphous soft phase, without showing any trace of crystallization or melting point. The glass transition temperature (T_g) varies between 6.6°C for the polyurethane prepolymer ZSMPU0 and 48.7°C for the sample with the highest sulfobetaine content, ZSMPU8 (heating: **Figure 2A**, cooling: **Figure S3**). Thus, grafting zwitterions leads to change in T_g from 26.6 to 48.7°C, making it suitable for biomedical applications due to their similarity to body or biomedical application temperatures. **Figure 2B** presents the weight loss upon heating, showing three stage degradation upon heating (**Figure 2B** and **Figure S4**). The first degradation stems from the urethane dissociation, mainly depending on the isocyanate and alcohol structures used³¹. The initial decomposition temperature (T_i), defined by a 5% weight loss, increases with rising MDEAPS-content. However, the second stage of degradation ($T=297-408^\circ C$) is related to cleavage of alcohols or soft segments²⁰, proving the lower thermal stability of MDEAPS-units than of MDEA-units. This finding

implies that sulfobetaine may negatively influence the thermal stability of soft segments or alcohols, a result that could be used to demonstrate the successful grafting of sulfobetaine in these ZSMPOs.

3.3 Dynamic mechanical properties

Figure 3.

The DMA-data ($\tan\delta(T)$, **Figure 3b**) prove that the transition identified in DSC (**Figure 2a**) is indeed the T_g , as a difference in modulus up to a factor of 300 is found (**Figure 3a**). The trend of T_g increasing with the increase of MDEAPS-content is confirmed. The fact that the materials become too soft to measure properly only above $\approx 120^\circ\text{C}$ proves the high molar mass of the samples and the absence of sizable crosslinking, assuming a long rubbery regime is the fingerprint of a high molecular un-crosslinked material³². The similarity of the changes around T_g for the ZSMPO2 to ZSMPO8 suggests that while the zwitterions significantly shift T_g , the chain dynamics themselves are mostly determined by chain stiffness and not by zwitterionic supramolecular interactions. All zwitterionic polyurethanes show a wide glass transition temperature range. e.g., 20°C - 85°C for ZSMPO2 and 35°C - 108°C for ZSMPO8. This broad glass transition was also reported in the perfluorosulfonate ionomer and the polyethylene-based carboxylated ionomer,^{4, 25} The possible reason is that the strong ionic interaction among the side chains greatly influence the mobility of backbone. The slow dissociation of ionic clusters or the creep relaxation of side chains upon heating makes polymer show a broad glass transition. The broad glass transition can be viewed as the collective contribution of an infinite number of transitions, each corresponding to infinitely sharp transition temperatures continuously distributed across the broad transition.⁴ According to previous reports on structure design for multi-shape-memory polymers,^{3, 4} it can be expected that the ZSMPOs also have multi-shape-memory behaviour. Additionally, a second relaxation attributed to the hard segment formed among urethane groups is also detected at high temperature. Similar to the T_g trend, the second transition shifts to higher temperature as the MDEAPS-content increases. The clear shoulder peaks in the $\tan\delta(T)$ curve confirm the formation of micro-phase separation structure when the MDEAPS-content is lower than 31.89wt%, e.g. ZSMPO2, ZSMPO4 and ZSMPO5. A higher frequency and lower heating rate (e.g. 10Hz and 1.0K/min) could make the second relaxation more clear in the $\tan\delta(T)$ curve (**Figure S 5**). A typical AFM image further confirms the formation of micro-phase structure composed of hard phase and soft phase in the ZSMPOs (Figure 3C-D). Together with the height 3D images (Figure C) and phase 3D images (Figure D), some cuspidal outshoots appear throughout the surface, which may be aggregation of the zwitterions serving as hard phase¹⁸. Whereas, the overlap of T_g peak and shoulder peak implies the phase mixing when the MDEAPS-content is higher than 37.07wt%, e.g. ZSMPO6, ZSMPO8.

3.4 Tensile mechanical properties

Figure 4.

Tensile mechanical properties of zwitterionic polyurethanes with different MDEAPS-content help the understanding of structure and morphology. Polyurethane without MDEAPS units (e.g. ZSMPU0) is an elastic polymer having low tensile strength and high elasticity, while ZSMPU8 shows brittle behaviour with no yields (Figure 4A). Both breaking strength and elongation at break increase with the increase of MDEAPS-content or molar ratio of PS/MDEA (Figure 4B). Tensile mechanical properties thus confirm the important role of zwitterions on the morphology of polyurethanes. Ionic clusters among MDEAPS reinforce the polyurethane serving as organic fillers. Zwitterionic polyurethane tends to show well-diffused micro-phase separation morphology composed of amorphous continuous soft phase and amorphous zwitterions-rich domains when the MDEAPS content is lower than 37.07wt%, whereas the continuous soft phase may be separated into drop-like phase when the MDEAPS-content is much higher, e.g. above 46.51wt%, displaying brittle fracture at ambient temperature. Therefore, glass transition of amorphous soft phase shifts to higher temperature as the MDEAPS content increases as discussed in DSC analysis. Increasing MDEAPS-content leads to the increase of phase mixing as identified in DMA analysis. However, it should be pointed out that the ionic interaction is mainly formed among side chains. Hydrogen bonding between urethane groups on the backbone was greatly destroyed by these ionic clusters. Therefore, shape memory effects of zwitterionic polyurethane should be quite different from the previous segmented polyurethanes.

3.5 Shape memory behaviours

Figure 5.

Figure 5 shows some of the obtained data proving the dual-, triple-, and quadruple–shape-memory effects. Figure 5A demonstrates that ZSMPU2 could be deformed to approximately 100% strain when the sample was heated to 60°C. After cooling below 0°C, almost all deformation was fixed. More than 90% strain recovery occurs when reheating to the deformation temperature. This is typical dual-shape memory behaviour. Moreover, this shape memory effect can be repeated, and the good shape fixity or shape recovery can be maintained for many times (Figure 5A). The other ZSMPUs with different MDEAPS-content also show similar dual-shape memory behaviour, ignoring the application temperature. (Figure S6). Overall, increasing MDEAPS-content leads to a decrease of shape recovery, despite good shape fixity for all samples (Figure 5B). One reason is that MDEAPS disturbs the hydrogen bonded physical cross-linking of ZSMPU serving as netpoints for shape

recovery³³, since FT-IR showed decreased H-bonding between urethane groups with increased MDEAPS-content. Another possible reason is that the strong electrostatic inter/intra-chain associations among MDEAPS promote the phase mixing, destroying the elasticity of polymer chain, since DMA demonstrated increased phase mixing with increased MDEAPS-content. This phenomena is very similar to the effects of hard segment in the common shape memory polyurethane, in which shape recovery decreases with the increase of hard segment content.⁹ Additionally, the triple-shape-memory effects of ZSMPU2, ZSMPU4 and ZSMPU5 (**Figures 4C-E**) are very good as demonstrated by the ability to fix two temporary shapes and recovering them in a programmed fashion, which is shown in more detail in Supporting information (**Table S1**). Strain fixity in the first stage is lower than in the second stage for all ZSMPUs due to the higher fixing temperature and, consequently, higher chain mobility. Similarly, the strain recovery in the first stage is much higher than that in the second stage because the resulting recovery force in the first stage is much higher due to the lower recovery temperature³. Comparatively, similar to the dual-shape-memory effects, strain recovery in the first stage and, in particular, the total strain recovery decreases as the MDEAPS-content increases (**Table S1**). Shape fixity in both the first and the second stage increases with MDEAPS-content, because the T_g increases with the increase of MEDAPS content as discussed in the DSC analysis. Additionally, quadruple-shape memory behaviour of ZSMPU4 are both equally good when fixing the three temporary shapes at 73°C, 58°C, and 0°C, which are 91.60% recovered at 58°C, 73°C, and 88°C, respectively(**Figure 4F**). These deformation temperatures and fixing temperatures were set up on basis of the DSC T_g of ZSMPU4 (e.g.27.49°C). Furthermore, a group photos confirm the zwitterionic polyurethane can sequentially recover their original shape *via* several previously programmed temporary shapes (**Figure S7**). These observations make zwitterionic polyurethane good candidates for potential applications such as smart bandages or stimuli-responsive delivery vehicles.

3.6 hydrophilicity properties

Figure 6.

The improved hydrophilicity of ZSMPUs can be directly observed from the linear decrease in the contact angle of water (**Figure 6A**) with increasing MEDAPS-content from 89° to 55° for ZSMPU0 and ZSMPU8, respectively. Hence, polyurethane's hydrophobic surface can be made more hydrophilic by introducing sulfobetaines to the backbone or side-chain,²⁰ thus improving biocompatibility for biomedical applications. **Figure 6B** also demonstrates good moisture absorption for all ZSMPUs, with increasing zwitterion content due to increasing hydrophilicity (**Figure S8**), initially following Fick's second law²⁶. ZSMPU0 shows a rapid diffusion, while ZSMPU6 and ZSMPU8 show slower diffusion, most likely because of hydration shell

formation (see **Figure S9**). Within 125 min, moisture absorption saturation is reached (at 80%RH/30°C). This outcome confirms the influence of zwitterions of ZSMPUs on moisture absorption, resulting from the electro-static attraction of water molecules (induced hydration). This induced hydration may endow the zwitterionic polyurethanes with self-healing properties, similar to the self-healing of cementitious materials³⁴. This result also provides another possible means of triggering the shape memory effect of ZSMPUs with moisture at a suitable temperature, as water shifts the T_g due to increasing chain mobility,³⁵ which can be further tuned by the MDEAPS-content and moisture conditions. This issue will be further investigated in future research.

3.7 Self-healing properties

Figure 7.

Being different from previous systems^{8, 36}, self-healing properties are achieved in the present zwitterionic polyurethane by water or moisture induced hydration and dehydration at low temperature. **Figure 7A** presents the self-healing behaviour of zwitterionic polyurethane. ZSMPU8 (Figure 7A-a) was cut into two parts (Figure 7A-b). After applying suitable moisture conditions (30°C and 80%RH) for several minutes, the cut parts become very soft and sticky, making it possible to recombine the previously cut parts with slight pressure. Initially, the healing zone interface is visible (**Figure 7A-c & e**), which disappears after drying at 50°C for 2 hours (**Figure 7A-d & f**, see supporting information **video S1**). Furthermore, as shown in Figure 7B, the shape memory properties are preserved, as demonstrated by an E-shaped sample where the arms are bent around. This sample shows good shape fixity and recovery after applying proper heat treatment, confirming the coexistence of good self-healing and shape memory properties, which can be ascribed to supramolecular zwitterionic interactions that hold the sample together initially before the regular entanglement network can rebuild itself across the former cut to fully heal the structure. This mechanism can be further verified from their self-healable tensile mechanical properties. Repeated self-healing treatment was performed on sample ZSMPU8 (**Scheme 2**), similar to the procedure described in literature.³⁷ Strain-stress curves show that both the strength and elongation of the second self-healed ZSMPU8-2 are very close to that of the first self-healed ZSMPU8-1 and the original sample ZSMPU8-0 (**Figure 7C**). Thus, products made of zwitterionic polyurethane with self-healable properties are expected to be used repeatedly. For instance, the zwitterionic polyurethanes could be used as medical bandages or protect-biomaterials, replacing the usage of plaster bandages. Damages could be self-repaired by adding water and drying with only sunlight.

4. Conclusion

The present study proposes a new strategy to prepare zwitterionic multi-shape-memory polyurethanes from MDEA, HDI and PS. ATR-FTIR, ¹H-NMR and XPS spectra confirm the successful formation of ionic clusters in the zwitterionic polyurethanes. Dynamic mechanical properties and tensile mechanical properties both demonstrate the effect of ionic clusters serving as organic fillers. Structure, morphology, and other properties are investigated to understand the multi-shape-memory behaviour with good shape fixity. However, shape recovery decreases with increasing MDEAPS-content. In addition, immersing the sample in moisture conditions and drying at low temperature preserves shape-memory capabilities and demonstrates good repeatable self-healing properties. The improved hydrophilicity of zwitterionic polyurethane suggests that the self-healing mechanism is ascribed to the spontaneous attraction of zwitterions, followed by slower re-entanglement. Considering the following studies of biocompatibility, zwitterionic polyurethane with multi-shape memory properties and self-healing properties are expected to be used as good candidates of smart biomaterials.

Acknowledgements

This work was financially supported by the National Natural Science Foundation of China (grant No. 21104045); the Special Research Foundation of Shenzhen Oversea High-level Talents for Innovation and Entrepreneurship (Grant No. KQCX20120807153115869), Nanshan District Key Lab for Biopolymers and Safety Evaluation (No.KC2014ZDZJ0001A), the Natural Science Foundation of Guangdong (grant S2013010013056), the Collaborative Innovation and Technology Project for Shenzhen-Hong Kong Innovation Circle of Shenzhen city (grant SGLH20120926161415782), and the Science and Technology Project of Shenzhen City (grant JCYJ20140828163633993).

References

1. A. Lendlein, *Internat. J. Artif. Organs.*, 2011, **34**, 607-607.
2. M. C. Serrano and G. A. Ameer, *Macromol. Biosci.*, 2012, **12**, 1156-1171.
3. Y. Luo, Y. Guo, X. Gao, B.-G. Li and T. Xie, *Adv. Mater.*, 2013, **25**, 743-748.
4. T. Xie, *Nature*, 2010, **464**, 267-270.
5. Y. Wong, J. Kong, L. K. Widjaja and S. S. Venkatraman, *Sci. China Chem.*, 2014, **57**, 476-489.
6. W. Small, P. Singhal, T. S. Wilson and D. J. Maitland, *J. Mater. Chem.*, 2010, **20**, 3356-3366.
7. S. Chen, H. Yuan, S. Chen, H. Yang, Z. Ge, H. Zhuo and J. Liu, *J. Mater. Chem. A*, 2014, **2**, 10169-10181.
8. S. Chen, H. Yuan, H. Zhuo, S. Chen, H. Yang, Z. Ge and J. Liu, *J. Mater. Chem. C*, 2014, **2**, 4203-4212.

9. S. J. Chen, J. L. Hu, Y. Q. Liu, H. M. Liem, Y. Zhu and Y. J. Liu, *J. Polym. Sci. Poly. Phys.*, 2007, **45**, 444-454.
10. S. J. Chen, J. L. Hu, S. G. Chen and C. L. Zhang, *Smart Mater. Struct.*, 2011, **20**, 06500301-06500309.
11. S. J. Chen, J. L. Hu, Y. Q. Liu, H. M. Liem, Y. Zhu and Q. H. Meng, *Polym. Int.*, 2007, **56**, 1128-1134.
12. P. Singhal, W. Small, E. Cosgriff-Hernandez, D. J. Maitland and T. S. Wilson, *Acta Biomater.*, 2014, **10**, 67-76.
13. M. C. Serrano, L. Carbajal and G. A. Ameer, *Adv. Mater.*, 2011, **23**, 2211- 2215.
14. C. M. Yakacki, R. Shandas, C. Lanning, B. Rech, A. Eckstein and K. Gall, *Biomaterials*, 2007, **28**, 2255-2263.
15. C. M. Yakacki, R. Shandas, D. Safranski, A. M. Ortega, K. Sassaman and K. Gall, *Adv. Funct. Mater.*, 2008, **18**, 2428-2435.
16. F. Mo, F. Zhou, S. Chen, H. Yang, Z. Ge and S. Chen, *Polym. Int.*, 2014, DOI: 10.1002/pi.4814.
17. L. Chen, L. Wang, Z. M. Yang, J. Shen and S. C. Lin, *Chinese J. Polym. Sci.*, 2003, **21**, 45-50.
18. J. Huang and W. Xu, *Appl. Surf. Sci.*, 2010, **256**, 3921-3927.
19. J. Yuan, J. Zhu, C. H. Zhu, J. Shen and S. C. Lin, *Polym. Int.*, 2004, **53**, 1722-1728.
20. C. Ma, H. Zhou, B. Wu and G. Zhang, *ACS Appl. Mater. Inter.*, 2011, **3**, 455-461.
21. P. N. Coneski and J. H. Wynne, *ACS Appl. Mater. Inter.*, 2012, **4**, 4465-4469.
22. J. Cao, M. Yang, A. Lu, S. Zhai, Y. Chen and X. Luo, *J. Biomed. Mater. Res. A*, 2012, **101**, 909-918.
23. L. Sun and W. M. Huang, *Soft Matter*, 2013, **6**, 4403-4406.
24. K. Yu, T. Xie, J. Leng, Y. Ding and H. J. Qi, *Soft Matter*, 2012, **8**, 5687-5695.
25. R. Dolog and R. A. Weiss, *Macromolecules*, 2013, **46**, 7845-7852.
26. S. Chen, J. Hu and H. Zhuo, *J. Mater. Sci.*, 2011, **46**, 6581-6588.
27. R. M. Kasi, S. K. Ahn and P. Deshmukh, *Macromolecules*, 2010, **43**, 7330-7340.
28. C. Liu, H. Qin and P. T. Mather, *J. Mater. Chem.*, 2007, **17**, 1543-1558.
29. J. Leng, X. Lan, Y. Liu and S. Du, *Prog. Mater. Sci.*, 2011, **56**, 1077-1135.
30. C. Yang, K. Sun, J. Liu, H. Wang and Y. Cao, *Polym. Int.*, 2010, **59**, 1296-1302.
31. D. K. Chattopadhyay and D. C. Webster, *Prog. Polym. Sci.*, 2009, **34**, 1068-1133.
32. H. L. Frisch, *Polym. Eng. Sci.*, 1980, **20**, 2-13.
33. J. Hu and S. Chen, *J. Mater. Chem.*, 2010, **20**, 3346-3355.

34. D. Snoeck, K. Van Tittelboom, S. Steuperaert, P. Dubruel and N. De Belie, *J.Intel.Material Syst.Str.*, 2014, 25, 13-24.
35. W. M. Huang, B. Yang, L. An, C. Li and Y. S. Chan, *Appl.Phys. Lett.*, 2005, **86**, .
36. Y. Yang and M. W. Urban, *Chem. Soc. Rev.*, 2013, 42, 7446-7467.
37. P. Du, X. Liu, Z. Zheng, X. Wang, T. Joncheray and Y. Zhang, *RSC Adv.*, 2013, **3**, 15475-15482.

List of Table, Scheme and Figures

- Table 1. Compositions of zwitterionic shape memory polyurethane samples and their results from EA
- Scheme 1. Synthetic route of zwitterionic shape memory polyurethanes
- Scheme 2. Illustration for the self-healing process of zwitterionic shape memory polyurethanes
- Figure 1. Molecular structure analysis of zwitterionic shape-memory polyurethanes
- Figure 2. A) the second DSC heating scans and B) TGA curves of zwitterionic shape memory polyurethanes
- Figure 3. DMA curves of zwitterionic shape memory polyurethanes and a typical AFM image of sample ZSMPU4
- Figure 4. Tensile Mechanical properties of zwitterionic shape memory polyurethanes
- Figure 5. Multi-shape-memory behaviour of zwitterionic shape memory polyurethanes
- Figure 6. A) Contact angles for water as a function of zwitterion content. B) Moisture absorption curves under 80%RH and 30°C atmosphere
- Figure 7. Photos showing self-healing behaviours (A), shape recovery behaviours of self-repaired ZSMPU 8(B); and tensile mechanical properties showing repeated self-healing properties

Development of Zwitterionic Polyurethanes with Multi-Shape Memory Effects and Self-healing Properties

*Shaojun Chen**, *Funian Mo*, *Yan Yang*, *Florian-Johannes Stadler*, *Shiguo Chen*, *Haipeng Yang*,
*Zaochuan Ge**,

Shenzhen Key Laboratory of Special Functional Materials, Shenzhen Engineering Laboratory for Advanced Technology of Ceramics, College of Materials Science and Engineering, Shenzhen University, Shenzhen, 518060, China.

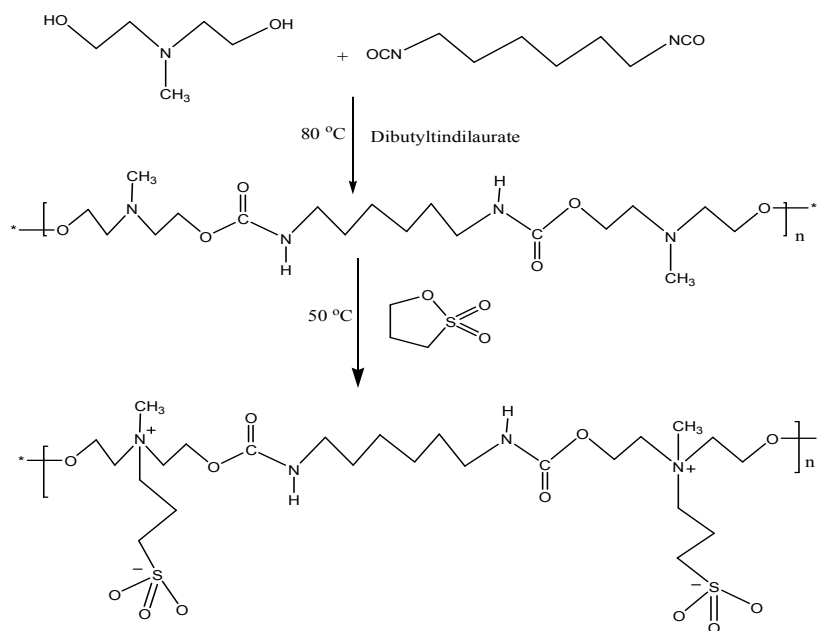
E-mail: S.J.Chen, chensj@szu.edu.cn; Z.C.Ge gezc@szu.edu.cn;

Figures, Tables and Schemes

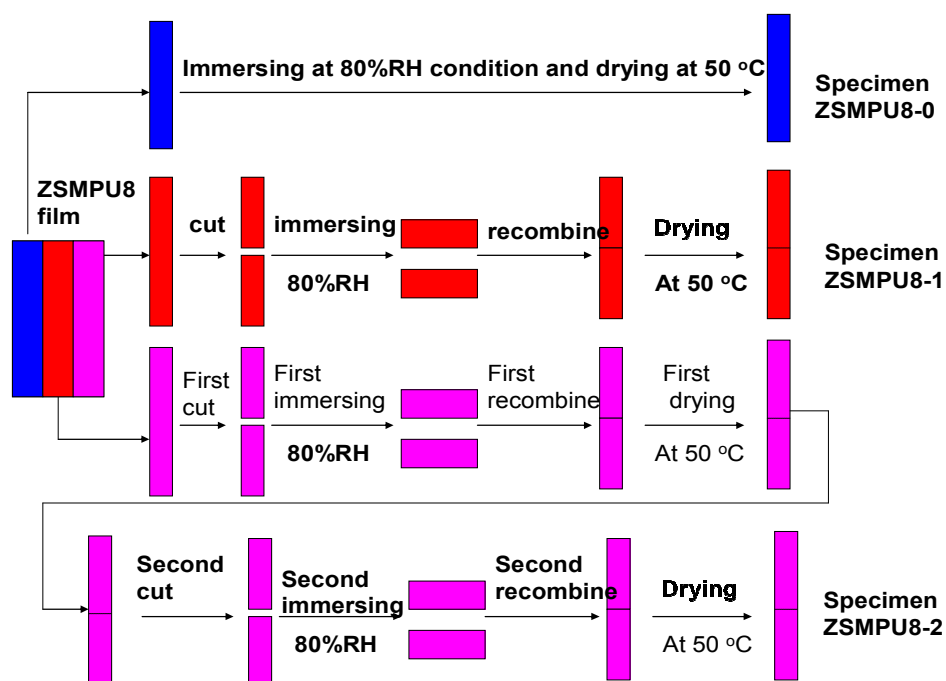
Table 1. Compositions of zwitterionic shape memory polyurethane samples and their results from EA

Samples	HDI (g)	MDEA (g)	PS/MDEA Molar ratio in feed	MDEAPS- content in feed (wt.%)	#MDEAPS- content by EA* (wt.%)	Elemental Composition (At. %)			
						N	C	H	S
ZSMPU0	34.5	20	0.0	0.00	--	14.94	57.89	8.43	0.01
ZSMPU2	34.5	20	0.2	14.12	11.16	12.44	50.30	7.27	1.48
ZSMPU4	34.5	20	0.4	26.36	20.89	11.75	48.89	7.25	2.77
ZSMPU5	34.5	20	0.5	31.89	28.28	11.30	48.39	7.40	3.75
ZSMPU6	34.5	20	0.6	37.07	33.03	11.01	47.85	7.49	4.38
ZSMPU8	34.5	20	0.8	46.51	41.40	10.25	46.45	7.55	5.49

*EA: Elemental Analyzer; # MDEAPS-content is calculated on basis of the S weight percentage obtained from EA.



Scheme 1. Synthetic route of zwitterionic shape memory polyurethanes



Scheme 2. Illustration for the self-healing treatment of zwitterionic shape memory polyurethanes

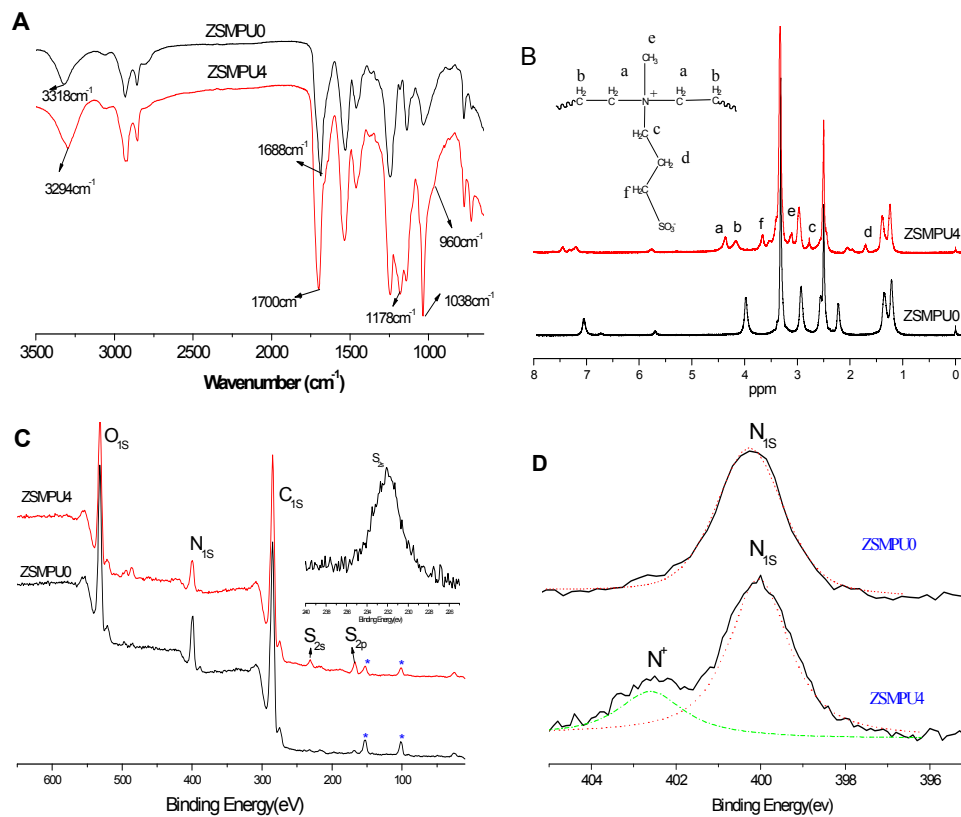


Figure 1. Molecular structure analysis of zwitterionic shape-memory polyurethanes (A) ATR-FTIR spectra; (B) $^1\text{H-NMR}$ spectra; (C) XPS spectra; (D) N_{1s} spectrum of ZSMPU0 and ZSMPU4)

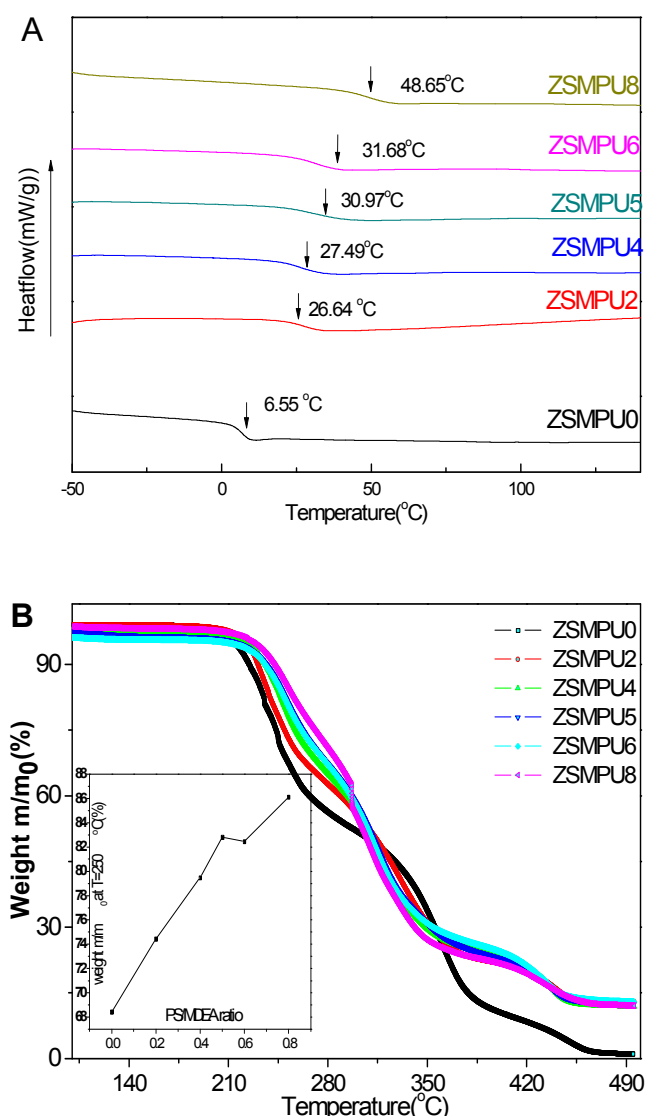


Figure 2. A) the second DSC heating scans and B) TGA curves of zwitterionic shape memory polyurethanes

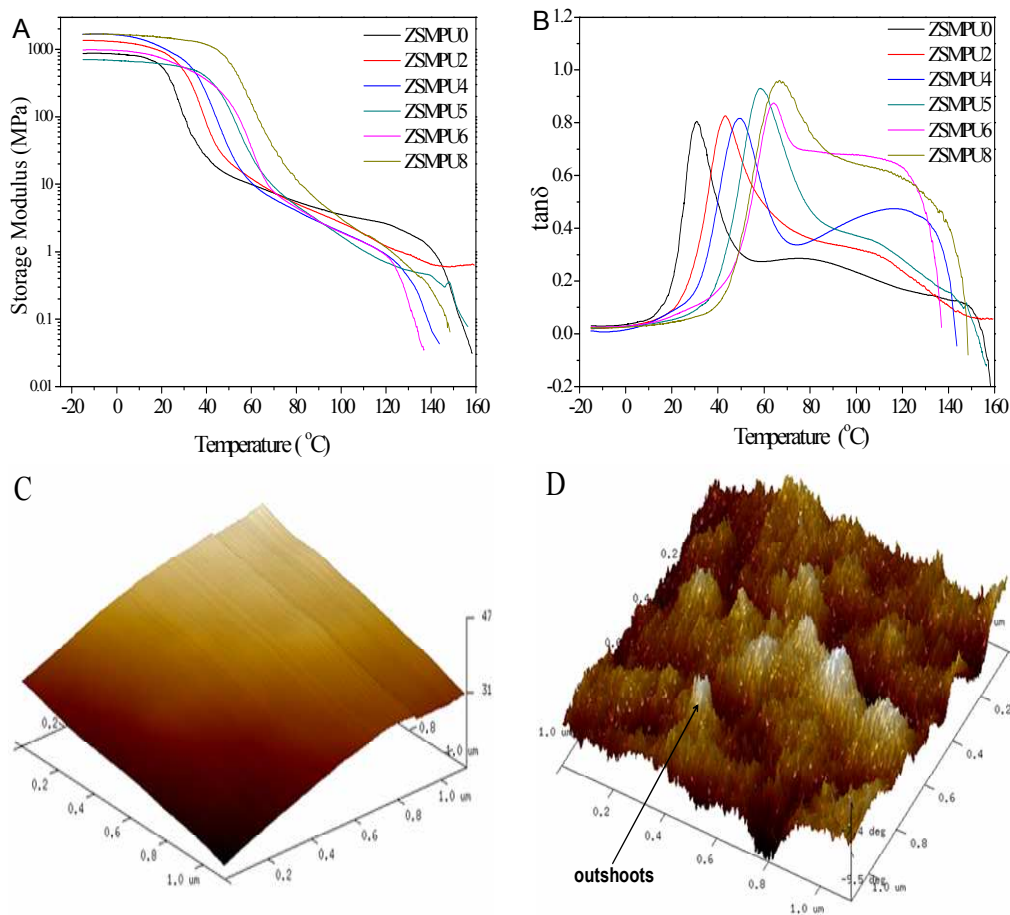
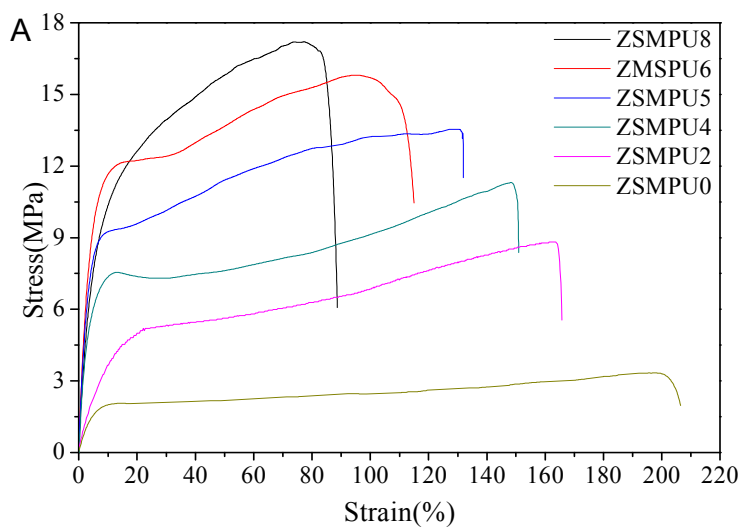


Figure 3. DMA curves (A) $E'(T)$; b) $\tan \delta(T)$ of zwitterionic shape memory polyurethanes; and Typical AFM images (C-height; D-phase) of sample ZSMPU4



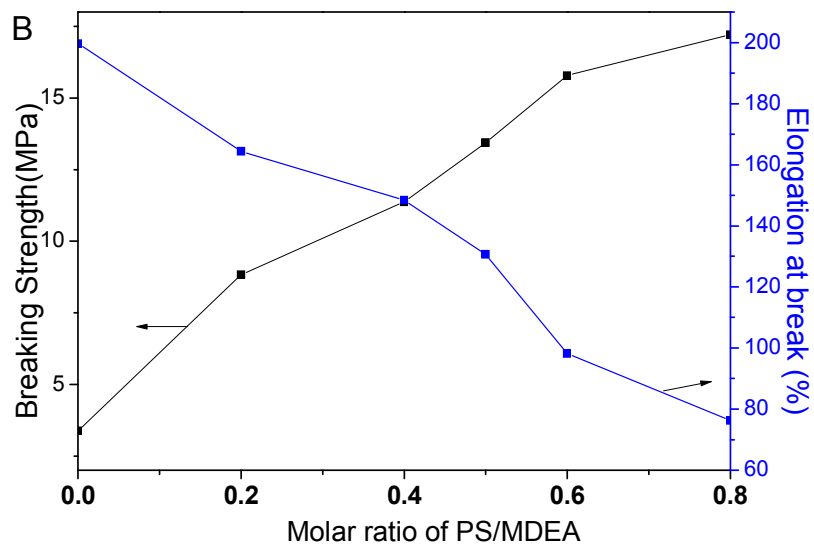
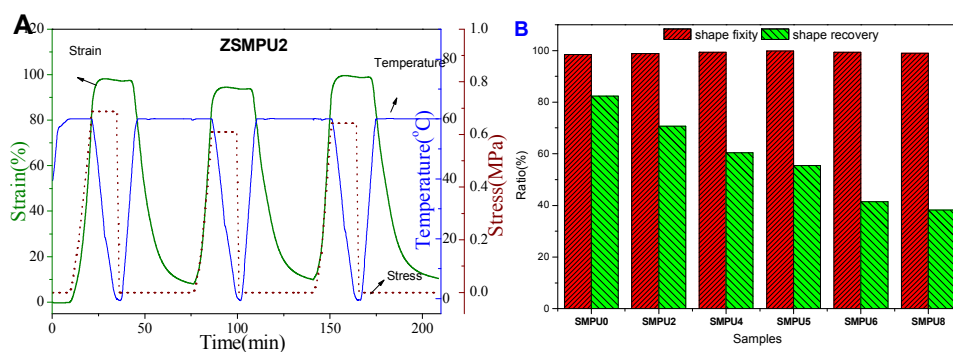


Figure 4. Tensile Mechanical properties of zwitterionic shape memory polyurethanes (A-strain-stress curves; B- Dependence of breaking strength and elongation at break on the molar ratio of PS/MDEA



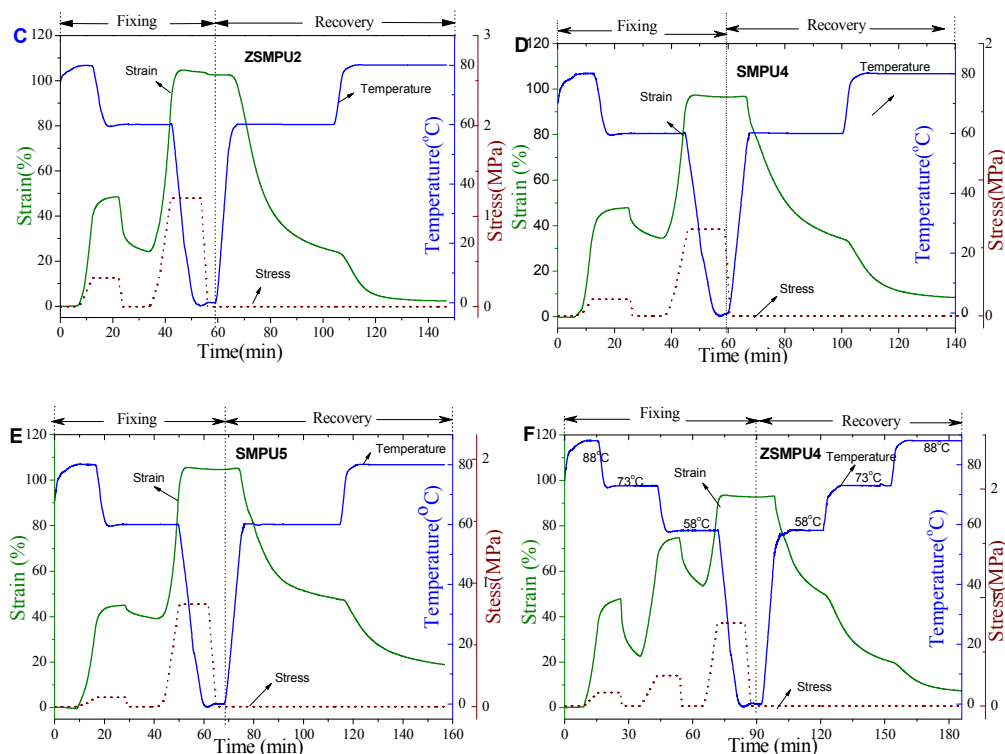
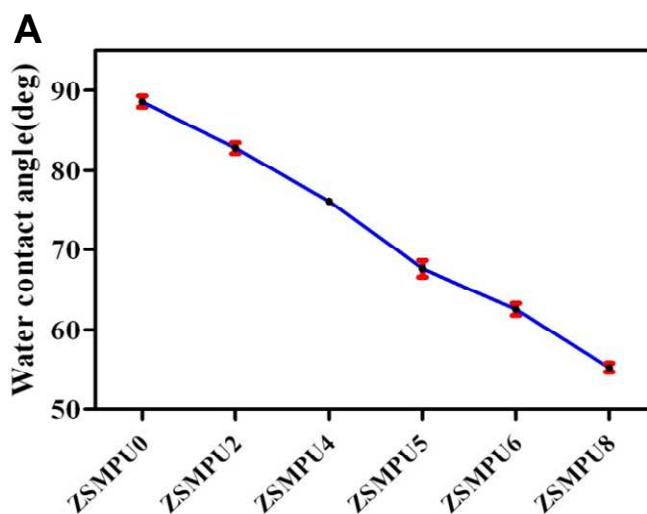


Figure 5. Multi-shape-memory behaviour of zwitterionic shape memory polyurethanes (A-repeatable dual-shape-memory behaviour of ZSMPU2; B-shape recovery and shape fixity for dual-shape-memory effects of ZSMPU samples; C-triple-shape-memory behaviour of ZSMPU2; D- triple-shape-memory behaviour of ZSMPU4; E-triple-shape-memory behaviour of ZSMPU5; F-Quadruple-shape-memory behaviour of ZSMPU4)



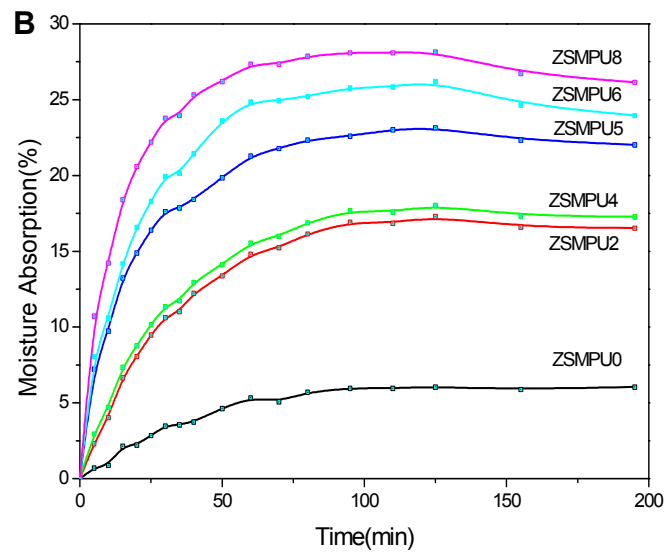
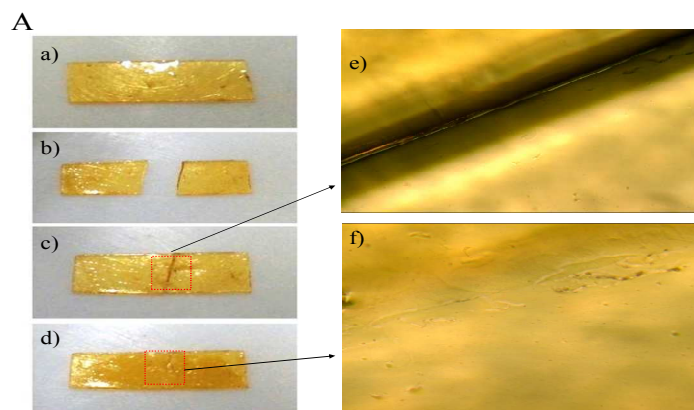


Figure 6. A) Contact angles for water as a function of zwitterion content. B) Moisture absorption curves under 80%RH and 30°C atmosphere



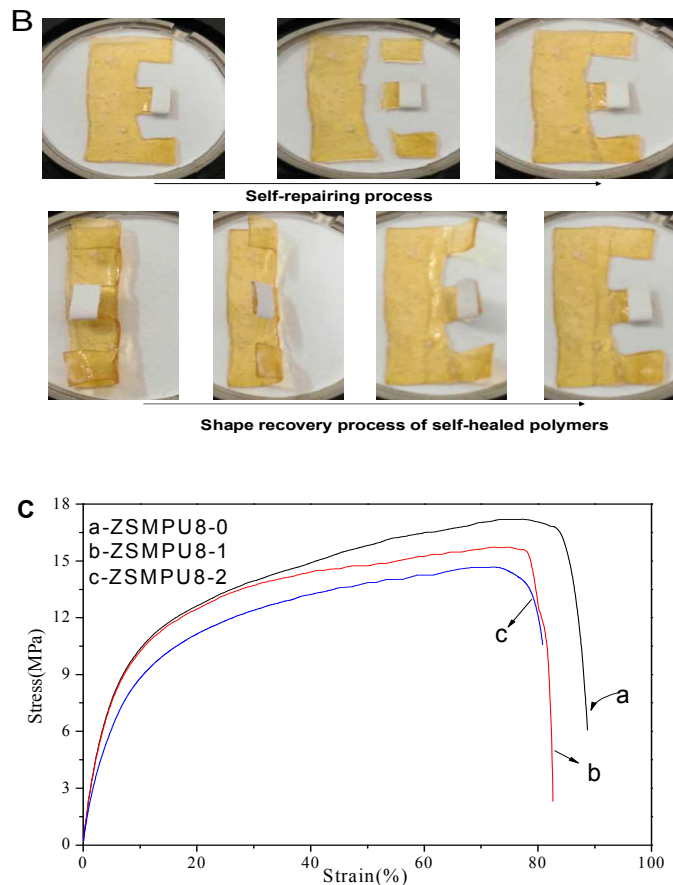


Figure 7. Photos showing self-healing behaviours (A) [a] original rectangle sample, b) rectangle sample was cut into two parts; c) cut parts were recombined slightly; d) self-healed sample; e) optical microscopy photo shows the healing zone's interface; f) the interface disappears on optical microscopy photo], shape recovery behaviours of self-repaired ZSMPU 8(B); and tensile mechanical properties showing repeated self-healing properties (a--its original sample ZSMPU8-0; b-the first healed sample ZSMPU8-1, c-the second healed sample ZSMPU8-2)

Development of Zwitterionic Polyurethanes with Multi-Shape Memory Effects and Self-healing

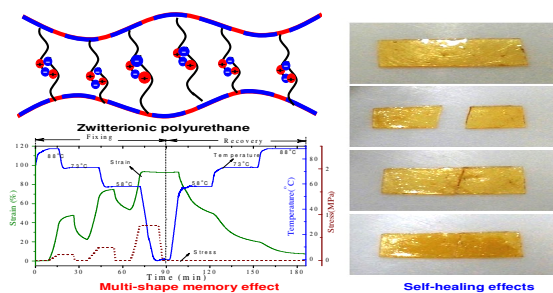
Properties

Shaojun Chen*, Funian Mo, Yan Yang, Florian-Johannes Stadler, Shiguo Chen, Haipeng Yang, Zaochuan Ge*

Shenzhen Key Laboratory of Special Functional Materials, Shenzhen Engineering Laboratory for Advanced Technology of Ceramics, College of Materials Science and Engineering, Shenzhen University, Shenzhen, 518060, China.

E-mail: S.J.Chen, chensj@szu.edu.cn; Z.C.Ge gezc@szu.edu.cn;

Graphic abstract



Novel zwitterionic polyurethanes containing sulfobetaines featured with excellent multi-shape-memory properties and self-healing properties are prepared from N-methyldiethanolamine, hexamethylene diisocyanate and 1,3-propanesultone.